

## Matrix Recharge of Vertic Forest Soil by Flooding

Savannah R. Morales<sup>1,2</sup>, Mary Grace T. Lemon<sup>1,3</sup>, Ryan D. Stewart<sup>4</sup>, and Richard F. Keim<sup>1</sup>

<sup>1</sup>School of Renewable Natural Resources, Louisiana State University, Baton Rouge, LA, USA.

<sup>2</sup>Providence Engineering and Environmental Group LLC, Baton Rouge, LA, USA. <sup>3</sup>US Fish and

Wildlife Service, Minneapolis, MN, USA. <sup>4</sup>School of Plant and Environmental Sciences,

Virginia Tech University, Blacksburg, VA, USA

Corresponding author: Richard Keim ([rkeim@lsu.edu](mailto:rkeim@lsu.edu))

### Key Points:

- Infiltration of floodwater via macropores ceased with swelling, but isotopic composition was heterogeneous even after 31 d of inundation
- Slow diffusion dominates isotopic evolution of soil moisture in Vertisols as porosity decreases
- The importance of flooding as a source of matrix recharge in vertic floodplain soils may depend more on flood frequency than duration

**18 Abstract**

19 Vertisols shrink and swell with changes in soil moisture, modifying hydraulic properties.  
20 Vertisols are often in floodplains, yet the importance of flooding as a source of soil moisture  
21 remains poorly understood. We used blue dye and deuterated water as tracers to determine the  
22 role of the macropore network in matrix recharge under artificial flood durations of 3 and 31 d in  
23 large soil monoliths extracted from a forested soil. Gravimetric soil moisture content increased  
24 by 47% in the first three days, then increased only 3.5% from day 3 to 31. Post-flood moisture  
25 content was greatest in the organic-rich, top 10 cm and was lower at 10 to 75 cm where organic  
26 matter was less. Deuterium concentration revealed that soil moisture in the top 10 cm was  
27 quickly dominated by artificial flood water, but at depth remained <80% floodwater even after  
28 31 d. Pervasive dye staining of ped surfaces in the top 4 cm indicated connectivity to flood  
29 waters but staining at depth was less and highly variable. The isotopic composition of soil water  
30 at depth continued to shift toward flood water despite no differences in dye staining between  
31 days 3 and 31. Results indicate flooding initially but incompletely recharges matrix water via  
32 macropores and suggest the importance of flooding as a source of matrix recharge in vertic  
33 floodplain soils may depend more on flood frequency than duration. Isotopic composition of  
34 matrix water in vertic soils depends on both advective and diffusional processes, with diffusion  
35 becoming more dominant as porosity decreases.

**36 Plain Language Summary**

37 Shrink-swell clay soils are common in floodplains but their behavior during flooding,  
38 particularly how much flood water they take up, is not well understood. We flooded large blocks  
39 of shrink-swell soil with artificial floodwater spiked with dye and chemically-labeled water, and  
40 found that water moved rapidly into soils via cracks and large soil pores, but swelling closed  
41 those pathways and prevented floodwater from spreading throughout the soil blocks. Only near  
42 the surface, where there is more organic matter, did floodwaters completely dominate soil  
43 moisture after flooding. Results indicate that flow into cracks in shrink-swell soil is important  
44 early in a flood, but not enough water flows this way to allow floodwater to reach throughout the  
45 soil before the clays swell and close those pathways. Because the amount of water that the soil  
46 can take up is limited in each event, the importance of flooding for soil moisture in shrink-swell  
47 clay soils in floodplains depends on how often flooding occurs rather than how long it persists.

## 48 **1 Introduction**

49 Fine-grained Vertisols are globally distributed and occupy approximately 2.4% of the earth's  
50 non-ice-covered surface (USDA-NRCS, 1999). Vertisols and related vertic intergrades are  
51 distinct because the smectitic clays that compose them impart shrink-swell properties that are a  
52 function of soil moisture (Groenevelt & Bolt, 1972; Das Gupta et al., 2006). At low moisture  
53 content the soil matrix shrinks, resulting in a heterogeneous network of cracks that readily  
54 transmit water in macropores. At high moisture content the matrix swells, partially closing the  
55 crack network and greatly reducing permeability. Thus, water flow paths are dynamic in both  
56 space and time (Stewart et al., 2015).

57  
58 In Vertisols, the cracks and slickensides that form the boundaries of soil pedes are macropores  
59 that conduct the majority of water, though not all macropores are connected and carry flow  
60 (Bouma et al., 1977; Yasuda et al., 2001). Vertic soils can become episaturated in some cases,  
61 meaning saturation of a surface- or near-surface layer and unsaturated below (Kishné et al.,  
62 2010). They can also develop local and discontinuous zones of saturation, affiliated with  
63 macropores, that do not necessarily connect to each other (Bouma et al., 1980; Armstrong 1983;  
64 Booltink & Bouma 1991). Upon wetting, cracks can close within hours (Favre et al., 1997) and  
65 shift hydraulic conductivity ( $K_{sat}$ ) from predominantly macropores flow to diffusional  
66 micropore flux (Bronswijk et al., 1995; Stewart et al., 2016b).

67  
68 Despite numerous studies and models devoted to quantifying matrix and macropore flow (e.g.,  
69 Flury et al., 1994; Hardie et al., 2013; Stewart et al., 2016), many hydrological processes in  
70 vertic clay soils remain poorly understood. For example, research to quantify vertic soil matrix  
71 recharge by precipitation has been extensive (e.g., Hoogmoed & Bouma, 1980; Römkens &  
72 Prasad, 2006), but the role of flood duration and ponding in soil moisture recharge has not been  
73 extensively investigated. Many vertic soils occur in current or former floodplains and lake  
74 bottoms, where landforms and topographic position are often conducive to flooding or ponding.  
75 Flooding plays a crucial role in influencing floodplain ecosystems through flood stress on plants,  
76 but it may also recharge soil moisture later used by plants (e.g., Lamontagne et al., 2005; Allen et  
77 al., 2016). Most field investigations of Vertisol hydrology under flooded conditions have focused  
78 on flux through the crack network (e.g., Bouma & Wösten, 1984) or on how the crack network is

79 modified by soil swelling upon ponding (e.g., Favre et al., 1997). There are reasons to expect the  
80 consequences of flooding for matrix moisture recharge may be larger than rainfall because  
81 flooding provides near-infinite water supply at high pressure potential, which can drive rapid  
82 infiltration through crack networks perhaps more rapidly than they can close. Alternatively,  
83 flooding may only induce limited recharge if matrix swelling closes cracks after infiltration of  
84 relatively small volumes of water. In the latter case, pre-event soil moisture may still dominate  
85 even after flooding.

86  
87 The enigmatic and poorly understood mechanisms controlling recharge of vertic soils have  
88 important implications for ecosystems. Soil moisture recharge, retention, and depletion are some  
89 of the most important processes governing ecosystem function. Most precipitation over land  
90 returns to the atmosphere as transpiration (Jasechko et al., 2013, Good et al., 2015), with  
91 moisture retention in the soil matrix acting as the primary store for this water. Water residence  
92 times in soil vary over many orders of magnitude, and transpiration tends to draw on older, rather  
93 than the most recently infiltrated, water (Berghuijs & Allen, 2019). This process creates a  
94 temporal decoupling between matrix recharge and uptake by plants, which can obscure sources  
95 of this important water store. Isotopic tracers have indicated separation between transpired water  
96 and younger water draining from soils in some cases (e.g., Brooks et al., 2010; Goldsmith et al.,  
97 2012; Allen et al., 2019), but mixing and isotopic exchange can complicate interpretations (e.g.,  
98 Oshun et al., 2016; Bowling et al., 2017; Vargas et al., 2017). Thus, considerable uncertainty  
99 remains about the hydrological sources of water available to plants in all soils, let alone in  
100 hydrologically complex, vertic soils.

101  
102 The goal of this research was to empirically quantify flood recharge of soil matrix water in a  
103 forested Vertisol, focusing on the role the macropore network plays in delivering water to the  
104 matrix. To do this, we conducted an artificial flooding experiment on soil monoliths transported  
105 intact to the laboratory. We used two tracers in our floodwater: (1) a sorbing, dye tracer to  
106 estimate connectedness of individual soil peds to the macropore network at multiple depths in the  
107 soil profile; and (2) a conservative tracer (deuterium) to estimate mass flux into peds. We  
108 hypothesized that soil peds most connected to the macropore network, as evidenced by dye-  
109 staining, would also attain the greatest isotopic enrichment.

## 110 2 Materials and Methods

### 111 2.1 Experiment Overview

112 We imposed artificial flooding on soil monoliths excavated intact from a forested Vertisol. The  
113 treatment monoliths were submerged in dyed and isotopically spiked water in short (3–4 days)  
114 versus long (31–32 days) artificial floods. After treatment, the monoliths were deconstructed to  
115 extract individual peds that were then analyzed for dye coverage, stable isotopic composition of  
116 soil water, moisture content, and organic matter content. Control monoliths were also  
117 deconstructed and analyzed for the same variables to quantify conditions prior to the artificial  
118 floods.

### 119 2.2 Field Sampling

120 The study site is in the floodplain of the Mississippi River near St. Gabriel, Louisiana (30°16'54"  
121 N, 91°05'21" W). Levees have prevented overbank flooding from the Mississippi River for more  
122 than 200 yr but the site is frequently inundated by ponded precipitation from late winter through  
123 spring. The mean annual precipitation is 158 cm and the mean annual temperature is 20°C. The  
124 site is occupied by a mixed-species floodplain forest dominated by *Celtis laevigata*, *Ulmus*  
125 *americana*, and *Fraxinus pennsylvanica*, with the last logging more than 60 yr in the past.

126  
127 The soil met the criteria for a Sharkey clay, a very-fine, smectitic, thermic Chromic Epiaquet.  
128 At the surface is an organic-rich horizon where there is little structure except for common, small,  
129 granular, “buckshot” (Broadfoot, 1962) aggregates. Below, the soil is composed of weak,  
130 medium (<30 mm) peds that are subangular and blocky or wedge-shaped with slickenside  
131 boundaries typical of Vertisols—the latter increasing below 20 cm. At the time of sampling in  
132 September 2018 (Figure 1), the soil was relatively dry and visibly cracked on the surface. Many  
133 fine- to medium-sized roots were present, especially in the top 40 cm; the largest root in any of  
134 the monoliths was ~1 cm diameter. Ped boundaries tended to be formed on sides of medium-  
135 sized roots, and there were no peds formed completely around medium roots. Fine roots ( $\leq 2$   
136 mm) were found within peds.

137

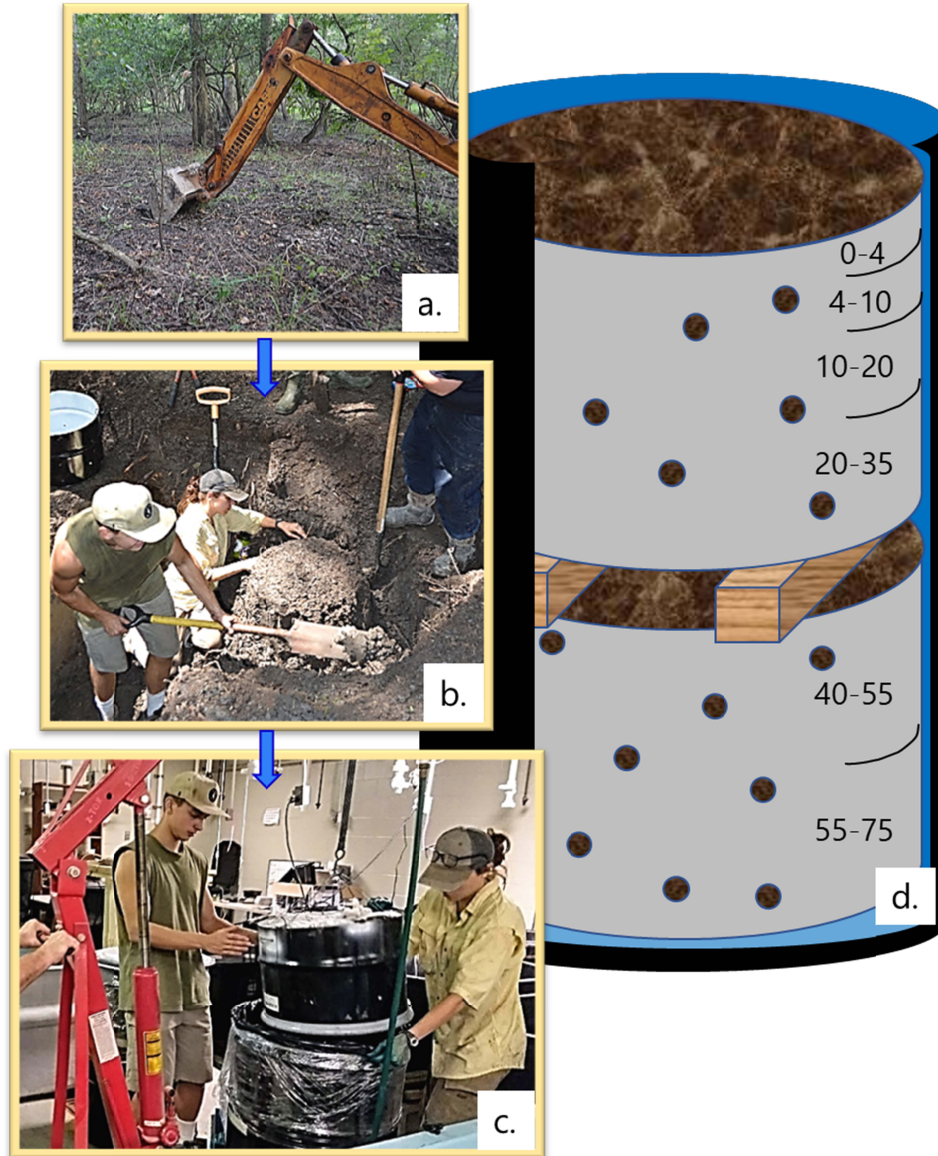
138 The monoliths each had a total volume of 62.5 L and were excavated in pairs from depths of 0–  
139 35 cm and 40–75 cm. Care was taken to ensure monoliths remained intact with as little  
140 disturbance as possible by gently excavating the soil surrounding the monolith while avoiding  
141 smearing until the desired size was achieved (Figure 1b). The monoliths were transferred to  
142 metal containers (each was one half of a 125 L steel drum, open on the top and pre-drilled with 1  
143 cm holes spaced 5–8 cm apart on the bottom and sides to allow relatively free movement of  
144 water) and wrapped in plastic and cushioned to prevent evaporation and stabilize the monoliths  
145 for transportation to the laboratory.

146

147 Two smaller, 19 L, control monoliths were also excavated from 0–35 cm and 40–75 cm depths  
148 and wrapped in plastic prior to transport to the laboratory. These monoliths were used to assess  
149 pre-flood soil properties.

150

151



152

153 **Figure 1.** Sampling and experimental setup: (a) initial excavation of a trench; (b) manual excavation of a  
 154 monolith adjacent to the trench—perforated sample container visible upper right; (c) lowering a monolith  
 155 into a tank of artificial floodwater.

156

157 **2.3 Artificial Flooding with Tracers**

158 In the laboratory, the soil monoliths were placed inside 208 L steel drums, with those excavated  
 159 from 40–75 cm depth placed on the bottom of the drums and the shallower monoliths placed on  
 160 top of them. Two 5 cm tall wooden spacers were used to separate upper and lower monoliths  
 161 (Figure 1d). This arrangement allowed for relatively high exposure to floodwaters of the external

162 portions of all monoliths, simulating networks of large macropores encompassing each monolith.  
163 Also, the perforated metal containers used to hold the monoliths constrained lateral expansion of  
164 the monoliths but allowed for vertical swelling at the surface of each monolith.

165  
166 To determine macropore-matrix connectivity and water exchange during flooding, two tracers  
167 were added to the flood treatment tanks prior to submerging the monoliths. Each tank contained  
168  $1 \text{ g L}^{-1}$  blue dye (variously known as FD&C Blue #1, C.I. 42090, Brilliant Blue FCF, and C.I.  
169 Food Blue 2) as a semi-quantitative, sorbing tracer of advective flux (Flury & Flühler, 1995;  
170 Ketelsen & Mayer-Windel, 1999; Öhrström et al., 2004). This is the common dye used in soil  
171 water flux tracing (Flury et al., 1994; Weiler & Flühler, 2004; Hardie et al., 2013), although we  
172 used a lower concentration due to a smaller ratio of soil volume to water volume as compared to  
173 most field experiments. Each tank was also spiked with deuterated water (98 atomic %) as a non-  
174 sorbing, conservative tracer of water movement. The initial soil water isotopic composition was  
175  $\delta D = +3\text{‰}$  at the surface,  $-5\text{‰}$  at 25 cm depth, and  $-15\text{‰}$  at 65 cm depth. The added floodwaters  
176 isotopic composition was  $\delta D = +68\text{‰}$  (tank with short-duration flooding) and  $\delta D = +70\text{‰}$  (tank  
177 with long-duration flooding). All isotopic values are reported per mil (‰) as  $\delta D =$   
178  $(R_{\text{sample}}/R_{\text{standard}} - 1) * 1000$ , where  $R = D/H$  in either the sample or Vienna Standard Mean Ocean  
179 Water (VSMOW).

180  
181 On the same day as excavation, the monoliths were fully submerged in the spiked floodwater,  
182 simulating a flood of  $\sim 3$  cm depth above the soil surface. The large drums were sealed to prevent  
183 evaporation and isotopic fractionation. After 3 days, one shallow monolith was removed from  
184 the floodwaters, and the paired, deeper monolith was removed one day later. Monoliths for the  
185 long-duration artificial flooding treatment were removed after 31 (upper monolith) and 32 (lower  
186 monolith) days.

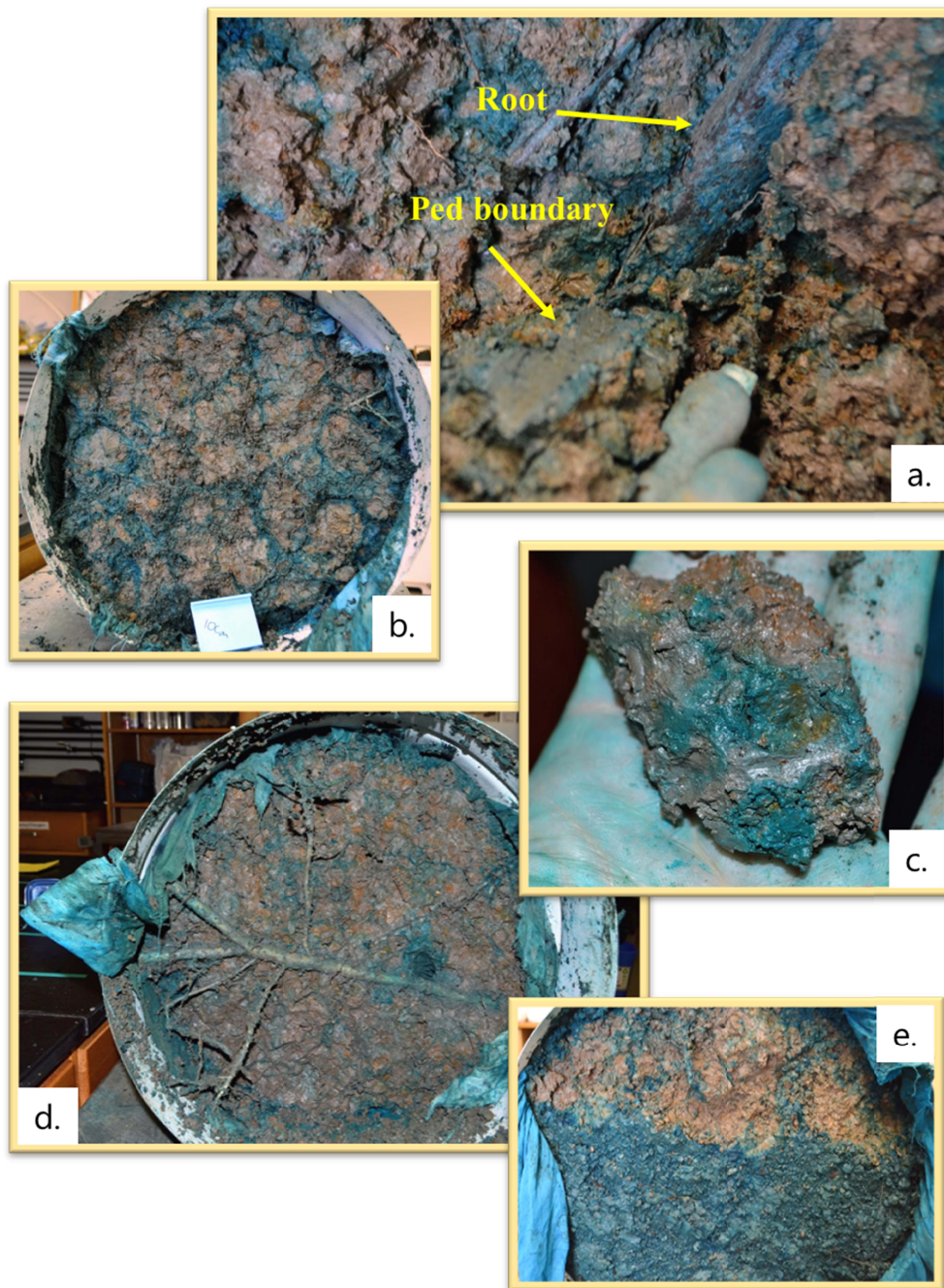
## 187 2.4 Soil and Water Sampling

188 Upon removal from the drums, monoliths were each allowed to freely drain for 20 minutes.  
189 Next, the thin ( $< 1$  cm) layer of litter at the surface and exterior soil,  $\sim 2$  cm on top, bottom, and  
190 sides was discarded as disturbed (except no soil was discarded from the top of the surface  
191 monolith). The remaining material was manually deconstructed by separating pedes along natural

192 lines of fracture to obtain treatment peds for analysis of dye coverage and  $\delta D$  (Figure 2). Ped  
193 excavation was performed using a knife tip and gently plucking out naturally structured peds.  
194 Peds that broke or appeared disturbed were discarded. Care was taken not to smear the soil or  
195 otherwise alter the ped surface. Also, care was taken to reduce evaporative fractionation of soil  
196 water by keeping the samples covered as much as possible and completing manual  
197 deconstruction within 11 hr.

198  
199 Peds were obtained from depth classes 0–4, 4–10, 10–20, 20–35, 40–55, and 55–75 cm. Soil  
200 properties in the upper 20 cm varied in structure more than below 20 cm, and smaller depth  
201 classes were designated there to account for this variability. Obtaining structured peds was also  
202 more difficult in the upper 20 cm due to high organic matter, and soil aggregates were smaller  
203 and more granular than the soil from deeper depths. Control peds were processed using the same  
204 methods as flood peds except depth classes were 0–4 cm, 4–35 cm, and 40–75 cm. Note that the  
205 methodology required peds of at least 3 g wet mass to provide sufficient water for isotopic  
206 analysis, so samples that did not meet this criterion were discarded. A total of 392 usable peds  
207 were collected, including 53 control peds, 162 short flood duration peds, and 177 long flood  
208 duration peds. Sampled ped size varied little by depth.

209



210  
 211 **Figure 2.** Dye staining revealed during deconstruction of monoliths: (a) stained root and adjacent ped  
 212 boundary illustrating preferential flow along roots; (b) top-down view of a monolith after the removal of  
 213 the surface 10 cm, illustrating preferential infiltration via a small proportion of the cross-section; (c)  
 214 manually removed ped illustrating partial dominance of slickensides and incomplete staining of ped  
 215 surface; (d) top-down view of a monolith after the removal of the surface 20 cm, illustrating a zone of  
 216 strong staining by preferential flow (center right) and common, but not ubiquitous, staining of the

217 rhizosphere; (e) top-down view of a monolith after partial removal of the top 4 cm, illustrating the rapid  
218 transition to highly preferential flow.

219

220 Once a ped was separated from a monolith, it was visually inspected for coverage of blue dye  
221 and assigned to a class of 0–20, 21–40, 41–60, 61–80, or 81–100 percent dye coverage.

222 Classification was done by the same person throughout the experiment to ensure consistency.

223

224 After dye coverage estimation, each ped was immediately placed into a sample bag for analysis  
225 of isotopic composition by equilibration with vapor (Wassenaar et al., 2008). Each bag was a 10  
226 L, side-gusseted metalized plastic coffee bag (PBFY Flexible Packaging; Gralher et al., 2018)  
227 that was inflated with ambient air, heat sealed, and incubated for isotopic equilibration between  
228 soil water and vapor for 2–3 days before analysis of the vapor by laser ablation spectroscopy  
229 (Los Gatos Research IWA–45–EP). Equilibration was in the same room as the isotope analyzer  
230 and recording thermometers (Onset HOBO) recorded the room temperature every 15 or 30  
231 minutes during this period to ensure consistency of temperature and thus equilibration between  
232 water and vapor. Bags containing liquid water standards for calibration were made on the same  
233 day as monolith deconstruction and equilibrated and analyzed following the same method as the  
234 ped bags. Precision of the  $\delta D$  in this experiment was  $\pm 1\%$ , estimated as the variance in values  
235 obtained by analyzing bags containing standards analyzed as samples.

236

237 To infer soil water  $\delta D$  from vapor  $\delta D$ , we used free-liquid  $\alpha$  (i.e., the temperature-dependent  
238 equilibration factor between vapor and liquid in a closed system), using recorded laboratory  
239 temperature and constants reported by Majoube (1971). We also performed an empirical control  
240 by analyzing vapor in the bags containing liquid water standards of known isotopic composition.  
241 We did not correct for fractionation known to occur by water sorbing onto surfaces (Lin and  
242 Horita, 2016; Lin et al., 2018; Oerter et al., 2014), by hydration spheres formed around solutes  
243 (Oerter et al., 2014), or by wetting of organic matter (Gaj et al., 2019). Comparing maximum  
244 measured soil-water  $\delta D$  (+79‰) to liquid  $\delta D$  in the submersion tanks after the experiment  
245 (+68‰ or +70‰), we estimated that ignoring effects of soil-surface and solute chemistry on our  
246 measurement may have caused error up to maximum 9‰, which is an order of magnitude  
247 smaller than the difference between pre-experiment water and the spiked floodwater (65–85‰).

248 Errors likely vary throughout the dataset because of varying mineralogy, solutes, and organic  
249 matter, so we report raw measurements instead of attempting corrections.

250

251 It is possible that isotopic equilibration between water in peds and in the vapor in the bags  
252 preferentially involved water near the surfaces of peds. If that were the case, the isotopic  
253 composition of the vapor may not have reflected the isotopic composition of the liquid in the  
254 entire ped. To assess this possibility, a separate experiment was conducted to test (1) whether the  
255 peds were fully equilibrating in the vapor bag during isotopic analysis and (2) whether any  
256 disequilibrium was related to ped size. Additional control and artificially flooded peds were  
257 processed using the same vapor bag equilibration methods as the main experiment, but with the  
258 exception that some peds (16 control and 22 treatment peds from soil soaked 24 h) were  
259 crumbled before being placed inside of the vapor bag and some (15 control and 22 treatment  
260 peds from soil soaked 24 h) were left whole and placed inside the vapor bags as for the main  
261 experiment. In the control group, there was no significant difference between the crumbled and  
262 whole peds (t-test  $p = 0.8$ , crumbled  $\delta D = -16 \pm 1\%$  s.d., whole  $\delta D = -16 \pm 1\%$ ). In the treatment  
263 group, there was high variance but no significant difference between the crumbled and whole  
264 peds (t-test  $p = 0.3$ , crumbled  $\delta D = +6 \pm 20\%$ , whole  $\delta D = 0 \pm 18\%$ ). The high variance in the  
265 treatment batch likely reflected the varying positions of the peds within the soaked soil monolith.  
266 Given these results, we concluded that sampling vapor equilibrated over whole, non-crumbled  
267 peds did not predictably bias the isotopic results, and that any plausible methodological effects  
268 were small relative to the difference between spiked, artificial floodwater and pre-treatment  
269 water.

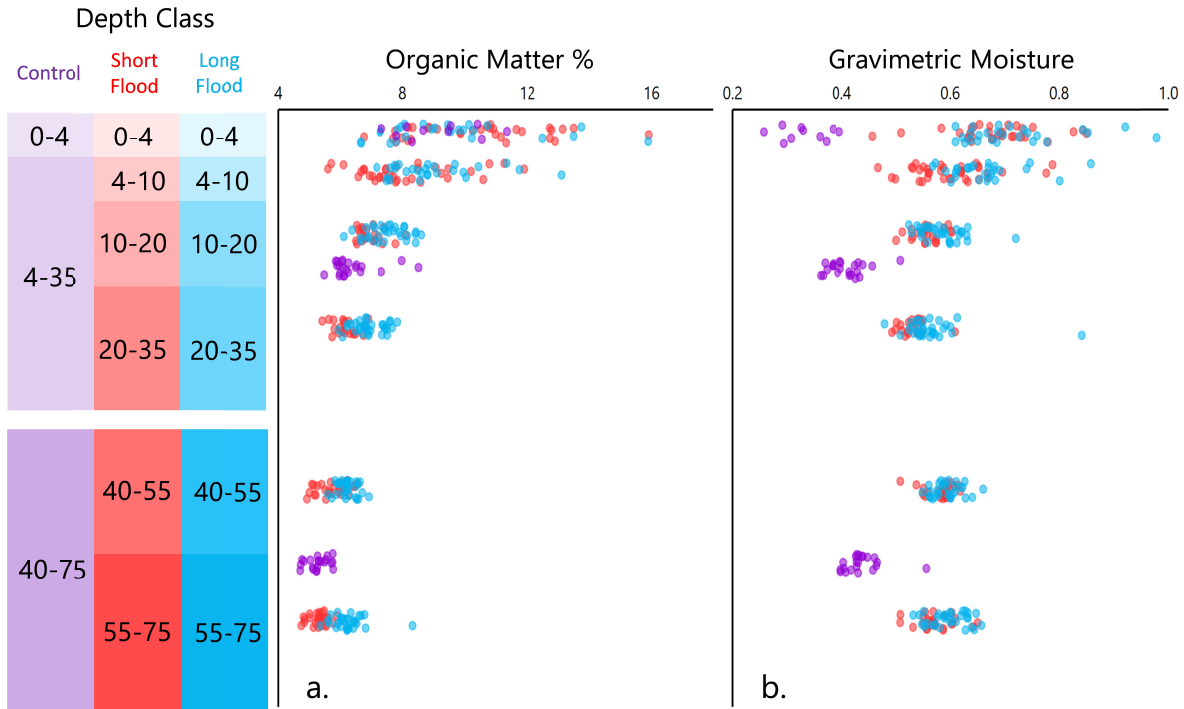
270

271 To infer the contribution of floodwater to ped moisture, we compared moisture content and  $\delta D$  in  
272 control and post-flood peds. For isotopic composition, we used a two-member mixing model as  
273  $\text{flood contribution} = (\delta D_{\text{ped, post-flood}} - \delta D_{\text{ped, pre-flood}}) / (\delta D_{\text{floodwater}} - \delta D_{\text{ped, pre-flood}})$ . There is  
274 uncertainty in pre-flood moisture content and  $\delta D$  because we used control peds to estimate those  
275 values rather than measuring the treated peds themselves, and there was additional, analytical  
276 uncertainty in  $\delta D$ , so we could make only coarse estimates of flood contributions. In the case of  
277  $\delta D$ , apparent flood contributions included mass flux of floodwater into peds as well as  
278 diffusional mixing of floodwater with pre-flood water.

## 279           2.5 Physical Properties of Peds

280   After measuring dye coverage and stable water isotopes, each ped (treatment and control) was  
281   measured for gravimetric moisture content (mass loss upon drying at 105°C as a proportion of  
282   oven-dry mass) and organic matter content (percent mass loss on ignition at 550°C). We  
283   quantified the size of peds by mass and moisture content gravimetrically because void ratio  
284   varies by moisture content in vertic clays and usurps the meaning of properties based on soil  
285   volume. Particle size analysis was performed on a 20 g mixed sample from each soil depth class  
286   Samples were prepared using mechanical and chemical deflocculation using sodium  
287   hexametaphosphate and removal of organic matter using H<sub>2</sub>O<sub>2</sub>. Prepared samples were then run  
288   through a laser diffraction particle size analyzer (S3500, Microtrac, Montgomeryville, PA, USA)  
289   assuming irregular particle shapes, transparent absorption coefficient, and a preset refractive  
290   index for clay (Özer et al., 2010; Jena et al., 2013). Soil texture was approximately 2% sand,  
291   60% silt, and 38% clay (Table B.1), using the USDA texture size classes of clay  $\leq 2.00 \mu\text{m}$ . The  
292   silt was very fine and most bordered on clay size: 15 percent of the particles were between 2 and  
293   3  $\mu\text{m}$ . Because particle size analysis using the laser diffraction method overestimates the size of  
294   particles as compared to the traditional sieve-pipette method (Beuselinck et al. 1998), it is likely  
295   that the clay fraction was underestimated. Organic matter decreased with depth across all peds  
296   (Figure 3a).

297



298

299

300 **Figure 3.** (a) Organic matter and (b) gravimetric moisture of control and artificially flooded soil peds.  
 301 Data were collected in depth classes and are presented with randomly jittered vertical positions for  
 302 visibility.

### 303 3 Results

304 Flooding caused gravimetric moisture content to increase across all depths from  $0.40 \pm 0.05$  g/g  
 305 (mean  $\pm$  SD) in the control peds to  $0.59 \pm 0.07$  g/g after the first 3–4 days, and then to  $0.62 \pm 0.08$   
 306 from 3–4 to 31–32 days (Figure 3b). Thus, artificial flooding contributed much more (47%  
 307 increase) at the onset of artificial flooding (i.e., the initial 3–4 days) than it did over the rest of  
 308 the flood period (5% additional increase). Gravimetric moisture content in the control soil  
 309 increased with depth but moisture content in the flooded peds decreased with depth after both  
 310 flood durations. Gravimetric moisture content increased for all depth classes from short to long  
 311 flood durations, although not statistically significantly at 0–4 cm (two-sample *t*-test;  $p = 0.166$ )  
 312 or 40–55 cm ( $p = 0.084$ ) depths. Due to experimental design, the surfaces of depth classes 0–4  
 313 cm and 40–55 cm both received greater exposure to treatment water and less confining pressure  
 314 from the surrounding soil than the other depth classes, thus providing more room for those peds  
 315 to expand and increase moisture. Gravimetric moisture in the control peds decreased with

316 organic matter content because the soil was drier at the surface, versus increased with organic  
317 matter content after both flood durations because the soil was wetter at the surface (Figure 3b).

318

319 In general, dye coverage on ped surfaces declined with depth for both flood durations (Figure 4).

320 Dye penetration did not occur more than a few mm into the soil matrix. For both artificial flood

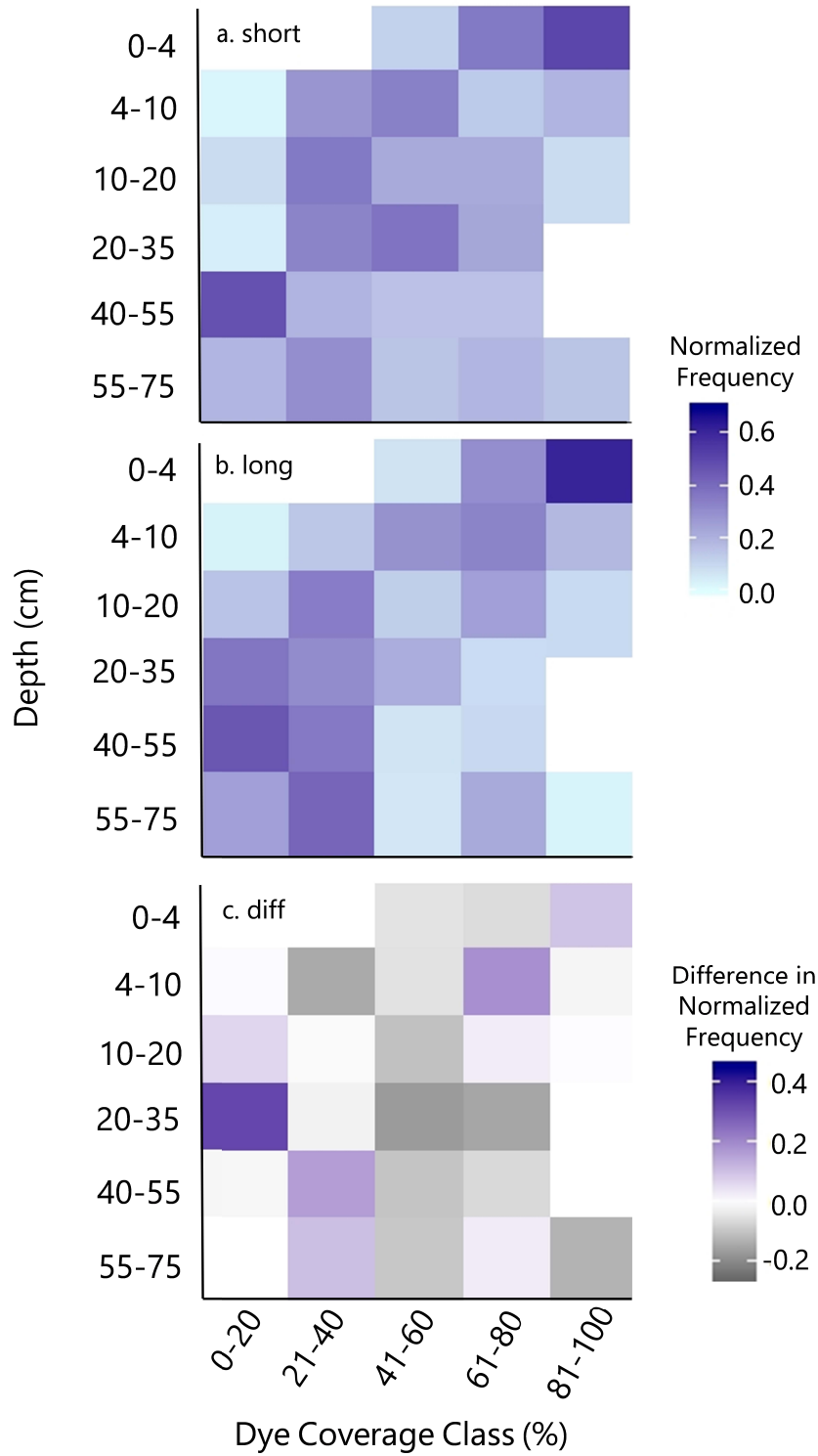
321 durations, dye coverage on surface peds was greatest in the 0–4 cm depth class and least in the

322 40–55 cm depth class (Figure 4a and b). There was no distinct pattern in differences of dye

323 coverage with depth between flood durations, but many depths showed no change or even

324 relatively less dye coverage for the long flooding event compared to the short (Figure 4c).

325

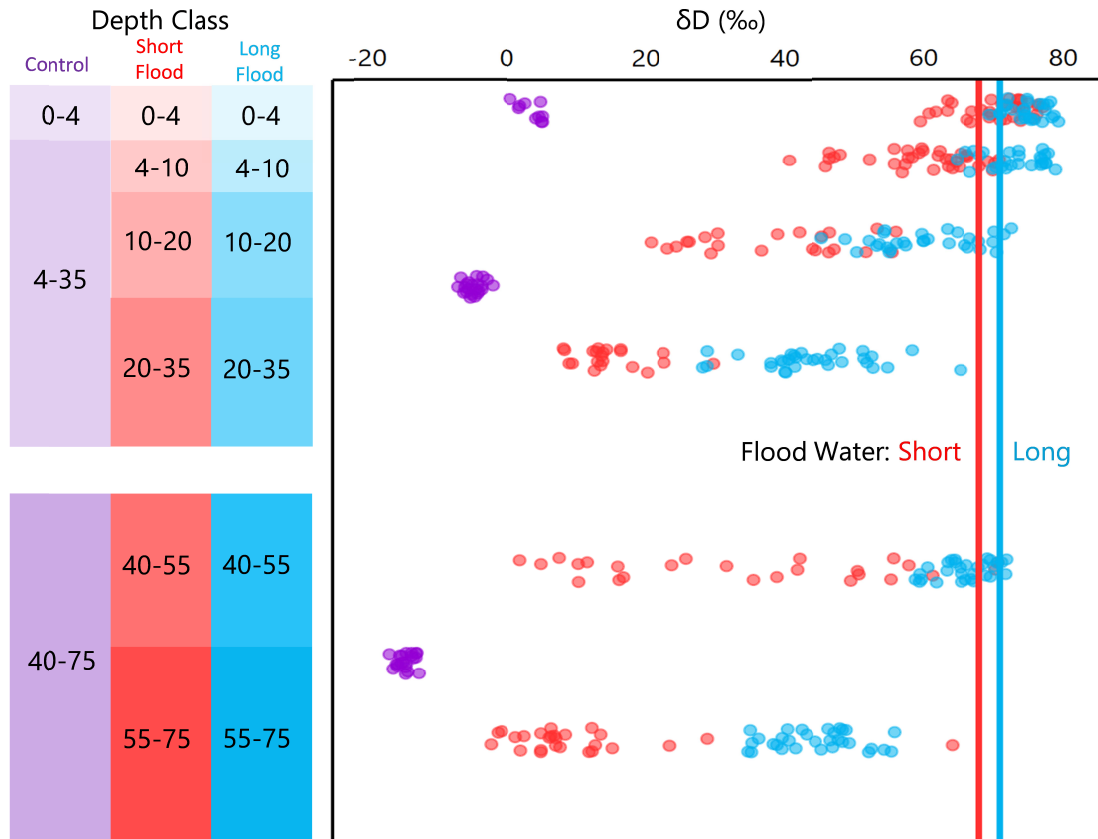


326

327 **Figure 4.** Normalized frequency of ped-surface dye-staining classes by depth class in the (a) short and (b)  
 328 long experimental floods and (c) the difference in frequency between the two durations of artificial  
 329 flooding.

330

331 In some peds, particularly those near the surface, deuterium concentration indicated pre-event  
332 water was almost completely replaced by flood water, but even after 32 days there was  
333 incomplete replacement of pre-event water at depth (Figure 5). After the short-duration flood,  
334 apparent isotopic contribution of the artificial flood water ranged from ~60–115% within 10 cm  
335 of the surface and mostly ~20–40% at depth. After the long-duration flood, apparent isotopic  
336 contribution of the artificial flood water exceeded ~90% within 10 cm of the surface and ~60–  
337 80% at depth. Ped water was more enriched in  $\delta D$  for the long flood duration (mean +59‰,  
338 compared to artificial floodwater of +70‰) than the short flood duration (mean +41‰,  
339 compared to artificial floodwater of +68‰) across all depth classes, indicating increasing content  
340 of artificial flood water in the ped matrix over time. The short-duration flooding was also  
341 associated with greater ranges of ped  $\delta D$ , indicating spatial variability in the absorption of flood  
342 water and diffusional exchange of deuterium. The smallest difference in  $\delta D$  between durations  
343 was at depth class 0–4 cm, where flood water dominated matrix water for both durations. In  
344 general, the differences in flood-water dominance between durations increased with depth. Ped  
345 water  $\delta D$  decreased with depth in the control peds (from +3‰ at the surface to -15‰ at 65 cm  
346 depth), yet those variations were small relative to the effects of the tracer addition.  
347



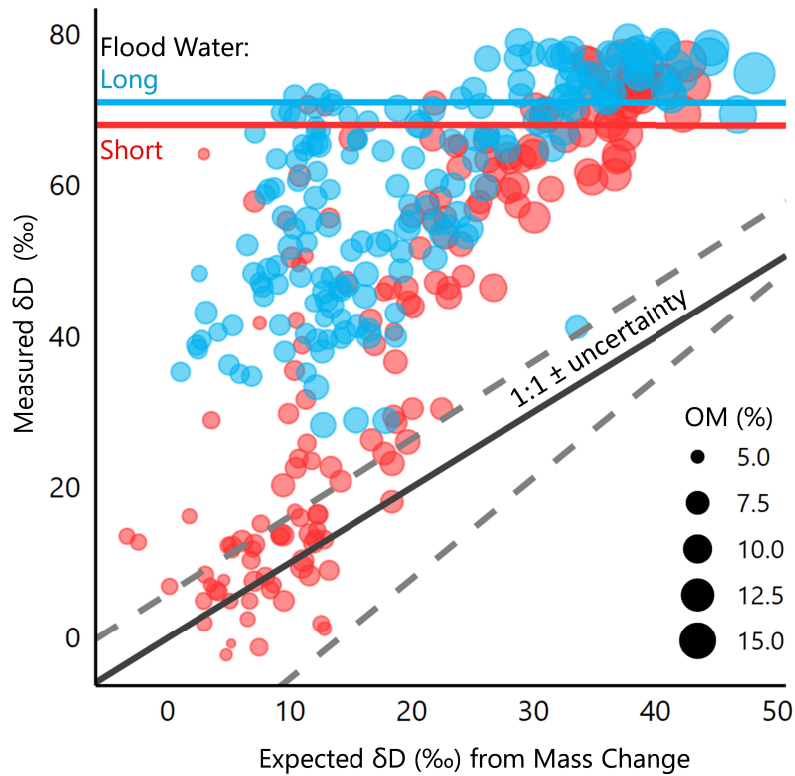
348

349 **Figure 5.** Concentration of deuterium in soil water from peds subjected to short- and long-duration  
 350 artificial flooding by water spiked with deuterium to the indicated concentrations. Data were collected in  
 351 depth classes and are presented with randomly jittered vertical positions for visibility.

352

353 Ped water  $\delta D$  was generally higher (i.e., more apparent flood water) than the expected  $\delta D$  given  
 354 mean moisture content differences between flooded peds and control peds (Figure 6). Isotopic  
 355 equilibration with the flood water was essentially complete (isotopic composition >90% of flood  
 356 water) for 30% of peds in the short-duration flood and 51% of peds in the long-duration flood.  
 357 Soil water  $\delta D$  in 25% of peds from the short-duration flood was within the bounds of expected  
 358  $\delta D$  given the mass change imparted by flooding and thus showed no evidence of equilibration by  
 359 diffusion beyond mass influx. These samples were clustered at the low end of measured (and  
 360 expected)  $\delta D$  values, indicating that these samples had limited wetting during the initial 3–4 days  
 361 of flooding. In contrast, all peds from the long-duration flood contained more deuterium than  
 362 expected given their increase in moisture content, indicating measurable equilibration with  
 363 experimental flood water. Isotopic equilibration was greater at the tops of the monoliths—where  
 364 expansion was least constrained—than it was at depth (Figure 5).

365



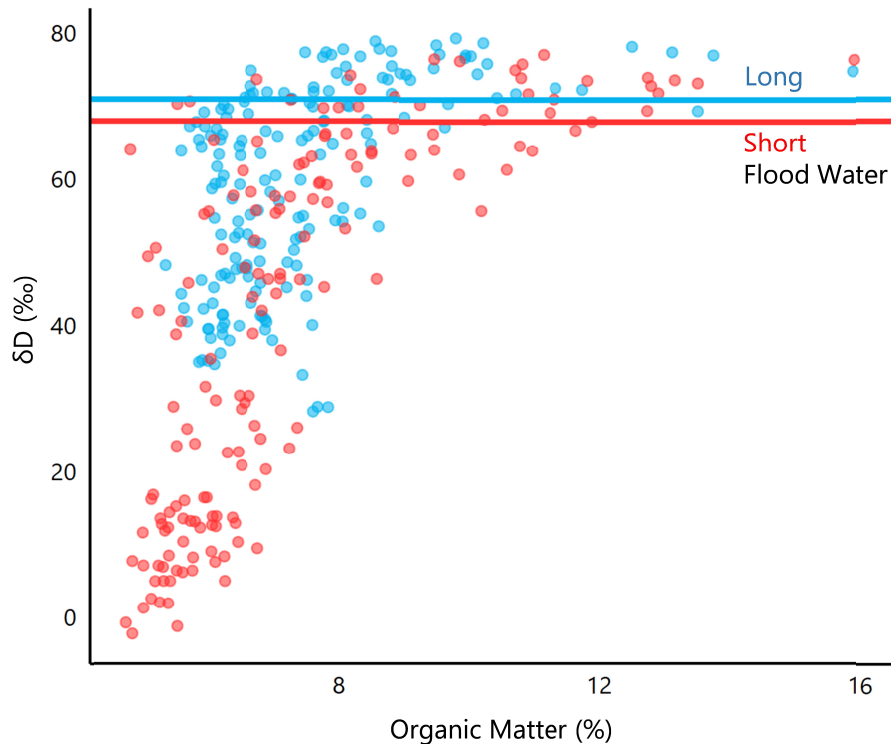
366

367 **Figure 6.** Deuterium concentrations in soil water compared to expected concentrations given deviation in  
 368 sample peds from mean moisture content and  $\delta D$  of control peds by depth. Dashed lines indicate bounds  
 369 of uncertainty, obtained by applying maximum or minimum observed  $\delta D$  and moisture content of control  
 370 peds by depth.

371

372 Much of the variance in ped-water  $\delta D$  was related to organic matter (Figure 7), likely because  
 373 peds containing more organic matter absorbed more flood water (Figure 3a). Ped-water  $\delta D$   
 374 increased with organic matter until the latter reached approximately 9% (Figure 7). Above 9%  
 375 organic matter, almost all peds were dominated by flood water and there was little variation of  
 376  $\delta D$ . The degree of equilibration (i.e.,  $\delta D$  greater than expected given mass influx alone) was not  
 377 clearly related to organic matter content (Figure 6).

378



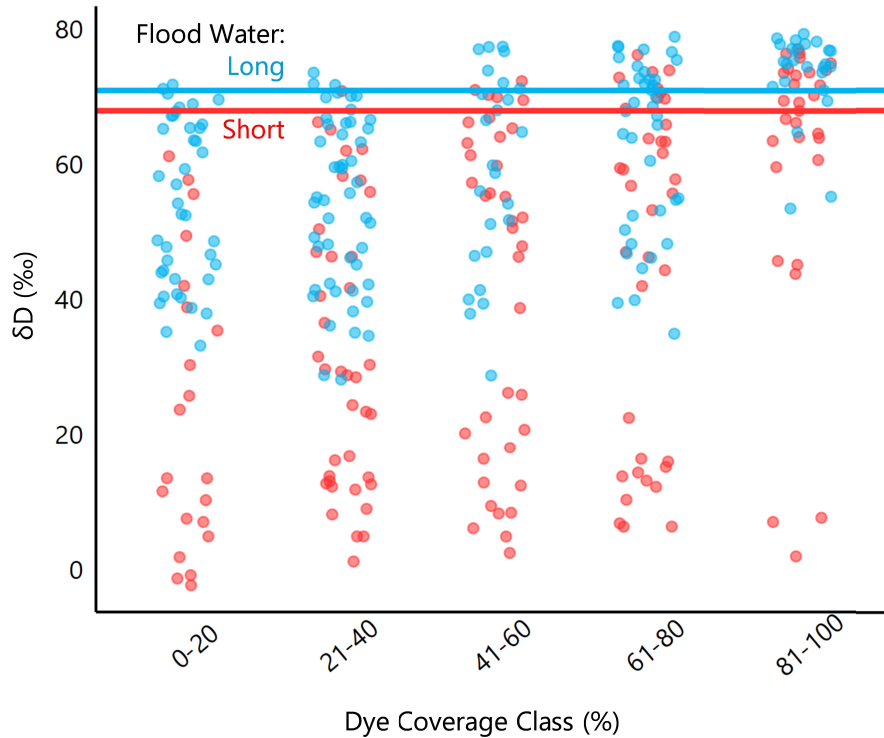
379

380 **Figure 7.** Concentration of deuterium in soil water from peds subjected to short- and long-duration  
 381 artificial flooding by water spiked with deuterium to the indicated concentrations, as a function of organic  
 382 matter per ped.

383

384 Deuterium concentration increased with dye coverage for both flood durations, although  
 385 variability among peds was high (Figure 8). Dye coverage was a poor predictor of  $\delta D$ , except  
 386 that peds completely covered by dye tended to be dominated by flood-event water. In the short-  
 387 flood treatment, water in 41% of peds remained less than 50% derived from the flood event,  
 388 including 10% of peds that were nearly completely covered by dye. Although dye coverage did  
 389 not increase between the short and long flood durations (Figure 4),  $\delta D$  continued to shift toward  
 390 flood event water with the longer flood duration. After the long-duration flood, 92% of peds that  
 391 were at least 80% covered by dye also contained more than 80% flood water.

392



393

394 **Figure 8.** Concentration of deuterium in soil water from peds subjected to short- and long-duration  
 395 artificial flooding by water spiked with deuterium to the indicated concentrations, as a function of dye  
 396 coverage per ped. Data were collected in dye coverage classes and are presented with randomly jittered  
 397 horizontal positions for visibility.

#### 398 **4 Discussion**

399 The vertic properties of our experimental soil had a strong apparent effect on moisture recharge  
 400 by flooding: soil moisture increased relatively little at depth as compared to the surface and  
 401 remained relatively constant after initial wetting even under continued inundation. The small  
 402 changes in water content at depth we observed are consistent with general soil moisture patterns  
 403 observed in other vertic clays in response to both flooding and rainfall. For example, Miller &  
 404 Bragg (2007) found relatively small differences in gravimetric moisture content at 100 cm  
 405 between soil under extended ponding and soil in prolonged seasonally dry conditions. Slabaugh  
 406 (2006) found relatively constant soil moisture with little apparent response to precipitation at  
 407 depths of 25–200 cm for two Vertisols in Mississippi, USA, over a 6-month period. There,  
 408 subsoil moisture content varied by only  $\pm 4\%$  annually, which is comparable to the 3% increase  
 409 found between the short and long artificial flood durations found in this experiment. Pettry &  
 410 Switzer (1996) reported consistent soil moisture despite precipitation variation in four Vertisols

411 in Mississippi, USA, over a 5-year period. They found the greatest moisture content and 80% of  
412 the total variation in soil moisture in the upper 50 cm.

413

414 Results indicate matrix recharge is a two-step process, beginning with rapid mass flux via  
415 macropores into peds during initial wet-up, followed by a period of isotopic equilibration  
416 between soil matrix and flood waters. The relatively unchanging moisture content and similarity  
417 of macropore connectivity (dye staining) between flood-duration treatments are consistent with  
418 many investigations of infiltration of rainfall into vertic soils, in which mass water flux declines  
419 rapidly because of crack closure (e.g., Favre et al., 1997). The subsequent increase in  $\delta D$  beyond  
420 expected concentrations from mass changes in our peds indicates that diffusion continued to be  
421 an important process after initial wet-up.

422

423 Many studies in floodplains and other low-lying agricultural soils have shown a longer-term  
424 swelling response when Vertisols become flooded. For example, Miller & Bragg (2007) found  
425 top-down, episaturation of field soil, with moisture content variation with depth, similar to our  
426 experiment, in both ponded and non-ponded forested Vertisols in Texas, USA. They reported  
427 that, during ponded conditions, ped interiors were wet ( $\geq 50\%$  gravimetric soil water content and  
428 soil glistened) down to 30 cm during the first two weeks of ponding and down to 50 cm after 3  
429 weeks. McIntyre et al. (1982) showed that swelling continued for several months as moisture  
430 slowly moved downward through the profile. These studies point to episaturation, in which near-  
431 surface layers become saturated before deeper ones, acting as a restriction on downward water  
432 movement and recharge.

433

434 In our experimental design the monoliths were submerged into flood waters, meaning that water  
435 could infiltrate from all directions. This approach reduced episaturation, and as a result the  
436 wetting behaviors observed in our study (rapid saturation followed by little change in water  
437 content) were more similar to those observed in studies conducted in well-structured upland clay  
438 soils where macropores give access through more of the soil profile (e.g., Stewart et al., 2015;  
439 Navar et al., 2002). At the same time, most of the change in soil water content in our experiment  
440 occurred in the uppermost layers. This result has analogs in several field studies of Vertisols,  
441 which showed that near-surface soils (e.g., the upper 50 cm) experience the majority of moisture

442 fluctuations under typical field conditions (Pettry & Switzer, 1996; Slabaugh, 2006; Miller &  
443 Bragg, 2007).

444  
445 Taken altogether, these results suggest that flood duration may be an important factor in water  
446 recharge for soils that quickly seal at the surface but is less important in soils with persistent flow  
447 pathways (e.g., root channels). For the latter, the frequency of flooding and drying cycles may  
448 instead represent a more important control on soil water recharge.

449  
450 By inhibiting episaturation, our experimental design allowed us to isolate relative effects of clay  
451 swelling, confining pressures, and OM on water movement in Vertisols. Soil moisture in  
452 Vertisols is strongly influenced by confining pressures within the soil that resist swelling and  
453 thus limit moisture (Groenevelt & Bolt 1972). Because the monoliths were divided into two  
454 pieces (0–35 and 40–75 cm), confining pressure was removed from the upper portion of the  
455 lower section. As a result, overburden pressure was low in both the 0–10 cm (i.e., 0–4 and 4–10  
456 cm) and 40–55 cm depth increments, yet these layers differed in OM (Figure 3a). The lack of  
457 confining pressure likely allowed greater increases in water content and  $\delta D$  in the 40–55 cm  
458 depth increment compared to the 20–35 cm depth (Figures 3b and 5). Likewise, there was much  
459 less variability in  $\delta D$  in the 40–55 cm depth class during the long artificial flood duration,  
460 suggesting that the greater swelling in that horizon facilitated greater isotopic exchange.  
461 However, the post-flooding water contents and mean  $\delta D$  of the 40–55 cm depth class were still  
462 lower than those at 0–10 cm, where there were many more fine roots, higher organic matter, and  
463 greater dye staining. Studies on bare soils have shown that surface crusting and sealing can force  
464 nearly all infiltrating water into cracks (e.g., Wells et al., 2003), but organic matter at the surface  
465 of our soil promoted infiltration into peds. Thus, OM appears to be important factor for mass flux  
466 and isotopic exchange in forested floodplain soils, regardless of flood duration.

467  
468 Dye coverage on ped faces was a poor predictor of isotopic composition of ped water after the  
469 artificial floods. From this, we conclude that infiltration into peds is also preferential, particularly  
470 deep in the soil profile where organic matter and porosity were lower and confining stresses  
471 resisting swelling were higher. Diffusion-driven water exchange caused the ped water to become  
472 more isotopically similar to the flood water through time. However, even after one month,

473 deeper peds continued to be depleted in D relative to the source water. While the exchange  
474 process likely would continue through time and eventually render a homogenous isotopic  
475 signature throughout, these results do suggest that soil water isotopes can resist mixing over  
476 short- to intermediate- timescales. The differences between the 20–35 cm depth class (median  
477  $\delta D$  of +42‰; ~66% event water) and 40–55 cm depth class (median  $\delta D$  of +65‰; ~91% event  
478 water) suggest that soil swelling likely also influences isotopic exchange. The swelling process  
479 allowed the soil peds to adsorb greater quantities of flood water (explaining the greater initial  $\delta D$   
480 increase in the 40–55 cm depth) and may have created bigger shifts in pore size distribution,  
481 which could facilitate more rapid exchange. Indeed, previous work has posited that small pores  
482 may be the most effective at retaining distinct pools of water (e.g., Sprenger et al. 2019).

483  
484 Our results are useful for interpreting whether there is distinct water pool partitioning between  
485 plant-available and runoff water—such as described by the “two water worlds” (TWW)  
486 hypothesis (Brooks et al., 2010)—in floodplain soils with shrink-swell properties. The  
487 interpretation of our results in terms of TWW depends on the mechanisms by which runoff  
488 occurs. If low permeability leads to dominance of episaturation, ponding, and surface runoff  
489 flowpaths, plant-available water is likely separate and dominated by the initial event water.  
490 However, ponding and surface runoff do not dominate all sites with vertic soils because cracking  
491 can lead to preferential flowpaths through soils to generate runoff from subsurface flowpaths  
492 (Allen et al. 2005). Also, even under saturated conditions, there may be continued subsurface  
493 flux through preferential pathways, such as root channels, that do not seal completely from  
494 swelling (Ritchie et al. 1972). Our results suggest that residence times of more than one month  
495 would be required for complete isotopic equilibration between runoff and plant-available water  
496 for the deeper soils, but that equilibration in the uppermost ~10 cm of floodplain Vertisols is  
497 likely to be rapid. Roots in this ecosystem are concentrated in the top ~20 cm of soil (Farrish  
498 1991) where moisture is most responsive to precipitation (Pettry and Switzer, 1996; Slabaugh,  
499 2006; Miller and Bragg, 2007), so water lower in the profile where equilibration is slower may  
500 not be important as direct plant water sources, and there may be little separation between runoff  
501 and plant-available water. To the degree that plants access water below the surface, organic-rich  
502 layer, there is likely to be strong separation between plant-available and runoff water in

503 Vertisols, but due to preferential flowpaths rather than the commonly cited reason of the soil  
504 moisture release curve (Brooks et al., 2010; Evaristo et al., 2015; Goldsmith et al., 2012).

## 505 **5 Conclusions**

506 Artificial flooding of soil monoliths revealed the processes by which inundation recharges soil  
507 matrix water in the presence of connected macropore networks. Soil water content increased  
508 rapidly in the initial three days of wetting, whereas over a subsequent four-week period  
509 molecular diffusion was the dominant mode of water exchange. There was a high degree of dis-  
510 connectivity between infiltrating flood and internal ped water, so there are some moisture stores  
511 of long residence time and low exchange with the more-rapid fluxes in the macropore network.  
512 Soil swelling and organic matter are both important factors controlling water flux into the soil  
513 matrix, so that near-surface peds quickly become dominated by event water but some deeper,  
514 confined peds with low organic matter may only exchange minor amounts of water. Macropores  
515 are active and dominate during the initial flood, but macropore flux ceases relatively quickly,  
516 resulting in diffusional processes recharging the matrix beyond initial wet-up. This poor  
517 connectivity of macropores to the matrix explains field observations of steady soil moisture,  
518 episaturation, and lack of connectivity between surface and subsurface water pools in vertic  
519 soils. We conclude that flooding has a rapid and large impact on soil moisture, but that neither  
520 the water nor chemistry of flood waters are comprehensively transmitted to the entire soil profile.

## 521 **Acknowledgments and Data**

522 United States Department of Agriculture (USDA) National Institute of Food and  
523 Agriculture, project LAB94374, provided financial support for research studies contributing to  
524 this manuscript. Funding for this work was provided in part by the Virginia Agricultural  
525 Experiment Station and the Hatch Program of the National Institute of Food and Agriculture ,  
526 USDA (1007839). Any opinions, findings, conclusions, or recommendations expressed in this  
527 publication do not necessarily reflect the view of the USDA. The authors declare no conflicts of  
528 interest. Data can be obtained from the USDA Ag Data Commons at  
529 <https://data.nal.usda.gov/dataset/data-matrix-recharge-vertic-forest-soil-flooding-0>.

530 **References**

- 531 Allen, P. M., Harmel, R. D., Arnold, J., Plant, B., Yelderian, J., & King, K. (2005). Field data  
532 and flow system response in clay (Vertisol) shale terrain, north central Texas, USA.  
533 *Hydrological Processes*, 19(14), 2719–2736. <https://doi.org/10.1002/hyp.5782>  
534
- 535 Allen, S. T., Krauss, K. W., Cochran, J. W., King, S. L., & Keim, R. F. (2016). Wetland tree  
536 transpiration modified by river-floodplain connectivity. *Journal of Geophysical Research*  
537 *Biogeosciences*, 121(3), 753–766. <https://doi:10.1002/2015JG003208>  
538
- 539 Allen, S. T., Kirchner, J. W., Braun, S., Siegwolf, R. T., & Goldsmith, G. R. (2019). Seasonal  
540 origins of soil water used by trees. *Hydrology and Earth System Sciences*, 23(2), 1199–1210.  
541 <https://doi.org/10.5194/hess-23-1199-2019>  
542
- 543 Armstrong, A. C. (1983). The measurement of watertable levels in structured clay soils by means  
544 of open augur holes. *Earth Surface Processes and Landforms*, 8(2), 183–187.  
545 <https://doi.org/10.1002/esp.3290080210>  
546
- 547 Berghuijs, W. R., & Allen, S. T. (2019). Waters flowing out of systems are younger than the  
548 waters stored in those same systems. *Hydrological Processes*, 33(25), 3251–3254.  
549 <https://doi.org/10.1002/hyp.13569>  
550
- 551 Beuselinck, L., Govers, G., Poesen, J., Degraer, G., & Froyen, L. (1998). Grain-size analysis by  
552 laser diffractometry: comparison with the sieve-pipette method. *Catena*, 32(3–4), 193–208.  
553 [https://doi.org/10.1016/S0341-8162\(98\)00051-4](https://doi.org/10.1016/S0341-8162(98)00051-4)  
554
- 555 Booltink, H.W.G., & Bouma, J. (1991). Physical morphological characterization of bypass flow  
556 in a well-structured clay soil. *Soil Science Society of America Journal*, 55(5), 1249–1254.  
557 <https://doi.org/10.2136/sssaj1991.03615995005500050009x>  
558

- 559 Bowling, D. R., Schulze, E. S., & Hall, S. J. (2017). Revisiting streamside trees that do not use  
560 stream water: Can the two water worlds hypothesis and snowpack isotopic effects explain a  
561 missing water source? *Ecohydrology*, *10*(1), e1771. <https://doi.org/10.1002/eco.1771>  
562
- 563 Bouma, J., Jongerius, A., Boersma, O., Jager, A., Schoonderbeek, D. (1977). The function of  
564 different types of macropores during saturated flow through four swelling soil horizons. *Soil*  
565 *Science Society of America Journal*, *41*(5), 945–950.  
566 <https://doi.org/10.2136/sssaj1977.03615995004100050028x>  
567
- 568 Bouma, J., Dekker, L. W., & Haans, J. C. F. M. (1980). Measurement of depth to water table in a  
569 heavy clay soil. *Soil Science*, *130*(5), 264–270.  
570
- 571 Bouma, J., & Wösten, J. H. M. (1984). Characterizing ponded infiltration in a dry cracked clay  
572 soil. *Journal of Hydrology*, *69*(1–4), 297–304. [https://doi.org/10.1016/0022-1694\(84\)90169-0](https://doi.org/10.1016/0022-1694(84)90169-0)  
573
- 574 Broadfoot, W. M. (1962). The fame of Sharkey clay. *Forests and People*, *12*(1), 30–31.  
575
- 576 Bronswijk, J. J. B., Hamminga, W., & Oostindie, K. (1995). Field-scale solute transport in a  
577 heavy clay soil. *Water Resources Research*, *31*(3), 517–526. <https://doi.org/10.1029/94WR02534>  
578
- 579 Brooks, J. R., Barnard, H. R., Coulombe, R., & McDonnell, J. J. (2010). Ecohydrological  
580 separation of water between trees and streams in a Mediterranean climate. *Nature Geoscience*,  
581 *3*(2), 100–104. <https://doi.org/10.1038/ngeo722>  
582
- 583 Das Gupta, S., Mohanty, B. P., & Köhne, J. M. (2006). Soil hydraulic conductivities and their  
584 spatial and temporal variations in a Vertisol. *Soil Science Society of America Journal*, *70*(6),  
585 1872–1881. <https://doi.org/10.2136/sssaj2006.0201>  
586
- 587 Farrish, K. W. (1991). Spatial and temporal fine-root distribution in three Louisiana forest soils.  
588 *Soil Science Society of America Journal*, *55*(6), 1752–1757.  
589 <https://doi.org/10.2136/sssaj1991.03615995005500060041x>

590

591 Favre, F., Boivin, P., & Wopereis, M. C. S. (1997). Water movement and soil swelling in a dry,  
592 cracked Vertisol. *Geoderma*, 78(1–2), 113–123. [https://doi.org/10.1016/S0016-7061\(97\)00030-](https://doi.org/10.1016/S0016-7061(97)00030-)  
593 X

594

595 Flury, M., Flühler, H., Jury, W. A., & Leuenberger, L. (1994). Susceptibility of soils to  
596 preferential flow of water: A field study. *Water Resources Research*, 30(7), 1945–1954.  
597 <https://doi.org/10.1029/94WR00871>

598

599 Flury, M. & Fluhler, H. (1995). Tracer characteristics of Brilliant Blue FCF. *Soil Science Society*  
600 *of America Journal*, 59(1), 22–27. <https://doi.org/10.2136/sssaj1995.03615995005900010003x>

601

602 Gaj, M., A. Lamparter, S.K. Woche, J. Bachmann, J.J. McDonnell, & C.F. Stange. (2019). The  
603 role of matric potential, solid interfacial chemistry, and wettability on isotopic equilibrium  
604 fractionation. *Vadose Zone Journal*,  
605 18(1), 180083. <https://doi.org/10.2136/vzj2018.04.0083>

606

607 Good, S. P., Noone, D., & Bowen, G. (2015). Hydrologic connectivity constrains partitioning of  
608 global terrestrial water fluxes. *Science*, 349(6244), 175–177.  
609 <https://doi.org/10.1126/science.aaa5931>

610

611 Goldsmith, G. R., Muñoz-Villers, L. E., Holwerda, F., McDonnell, J. J., Asbjornsen, H., &  
612 Dawson, T. E. (2012). Stable isotopes reveal linkages among ecohydrological processes in a  
613 seasonally dry tropical montane cloud forest. *Ecohydrology*, 5(6), 779–790.  
614 <https://doi.org/10.1002/eco.268>

615

616 Groenevelt, P. H., & Bolt, G. H. (1972). Water retention in soil. *Soil Science*, 113(4), 238-245.

617

618 Hardie, M., Doyle, R., Cotching, W., Holz, G., & Lisson, S. (2013). Hydropedology and  
619 preferential flow in the Tasmanian texture-contrast soils. *Vadose Zone Journal*, 12(4)  
620 <https://doi.org/10.2136/vzj2013.03.0051>

621

622 Hoogmoed, W.B., & Bouma, J., (1980). A simulation model for predicting infiltration into  
623 cracked clay Soil. *Soil Science Society of America Journal*, 44(3), pp.458–461.

624 <https://doi.org/10.2136/sssaj1980.03615995004400030003x>

625

626 Jasechko, S., Sharp, Z. D., Gibson, J. J., Birks, S. J., Yi, Y., & Fawcett, P. J. (2013). Terrestrial  
627 water fluxes dominated by transpiration. *Nature*, 496(7445), 347–350.

628 <https://doi.org/10.1038/nature11983>

629

630 Jena, R. K., Jagadeeswaran, R., & Sivasamy, R. (2013). Analogy of soil parameters in particle  
631 size analysis through laser diffraction techniques. *Indian Journal of Hill Farming*, 26(2), 78–83.

632

633 Ketelsen, H. & Meyer-Windel, S. (1999). Adsorption of brilliant blue FCF by soils. *Geoderma*,  
634 90(1–2), 131–145. [https://doi.org/10.1016/S0016-7061\(98\)00119-0](https://doi.org/10.1016/S0016-7061(98)00119-0)

635

636 Kishné, A. Sz., Morgan, C. L. S., Ge, Y., & Miller, W.L. (2010). Antecedent soil moisture  
637 affecting surface cracking of a Vertisol in field conditions. *Geoderma*, 157(3–4), 109–117.

638 <https://doi.org/10.1016/j.geoderma.2010.03.020>

639

640 Lamontagne, S., Leaney, F. W., & Herczeg, A. L. (2005). Groundwater–surface water  
641 interactions in a large semi-arid floodplain: implications for salinity management. *Hydrological*  
642 *Processes*, 19(16), 3063–3080. <https://doi.org/10.1002/hyp.5832>

643

644 Lin, Y., & Horita, J. (2016). An experimental study on isotope fractionation in a mesoporous  
645 silica-water system with implications for vadose-zone hydrology. *Geochimica et Cosmochimica*  
646 *Acta*, 184, 257–271. <https://doi.org/10.1016/j.gca.2016.04.029>

647

648 Lin, Y., Horita, J., & Abe, O. (2018). Adsorption isotope effects of water on mesoporous silica  
649 and alumina with implications for the land-vegetation-atmosphere system. *Geochimica et*  
650 *Cosmochimica Acta*, 223, 520–536. <https://doi.org/10.1016/j.gca.2017.12.021>

651

652 Majoube, M. (1971). Fractionnement en  $^{18}\text{O}$  entre la glace et la vapeur d'eau. *Journal de Chimie*  
653 *Physique et de Physico-Chimie Biologique*, 68, 1423–1436.

654 <https://doi.org/10.1051/jcp/1971680625>

655  
656 McIntyre, D., Watson, C., & Loveday, J. (1982). Swelling of a clay soil profile under ponding.  
657 *Soil Research*, 20(2), 71–79. <https://doi.org/10.1071/SR9820071>

658  
659 Miller, W. L., & Bragg, A. L. (2007). *Soil Characterization and Hydrological Monitoring*  
660 *Project, Brazoria County, Texas, Bottomland Hardwood Vertisols*. US Department of  
661 Agriculture, Natural Resources Conservation Service, Temple, TX (13 pp.).

662  
663 Oerter, E., Finstad, K., Schaefer, J., Goldsmith, G. R., Dawson, T., & Amundson, R. (2014).  
664 Oxygen isotope fractionation effects in soil water via interaction with cations (Mg, Ca, K, Na)  
665 adsorbed to phyllosilicate clay minerals. *Journal of Hydrology*, 515, 1–9.  
666 <https://doi.org/10.1016/j.jhydrol.2014.04.029>

667  
668 Öhrström, P., Hamed, Y., Persson, M., & Berndtsson, R. (2004). Characterizing unsaturated  
669 solute transport by simultaneous use of dye and bromine. *Journal of Hydrology*, 289(1–4), 23–  
670 35. <https://doi.org/10.1016/j.jhydrol.2003.10.014>

671  
672 Oshun, J., Dietrich, W. E., Dawson, T. E., & Fung, I., (2016). Dynamic, structured heterogeneity  
673 of water isotopes inside hillslopes. *Water Resources Research*, 52(1), 164–189.  
674 <https://doi.org/10.1002/2015WR017485>

675  
676 Özer, M., Orhan, M., & Işık, N. S. (2010). Effect of particle optical properties on size  
677 distribution of soils obtained by laser diffraction. *Environmental & Engineering Geoscience*,  
678 16(2), 163–173. <https://doi.org/10.2113/gseegeosci.16.2.163>

679  
680 Pettry, D. E., & Switzer, R. E. (1996). *Sharkey Soils in Mississippi*. Mississippi Agriculture and  
681 Forestry Experiment Station Bulletin 1057 (37 pp.).

682

- 683 Ritchie, J. T., Kissel, D. E., & Burnett, E. (1972). Water movement in undisturbed swelling clay  
684 soil. *Soil Science Society of America Journal*, 36(6), 874–879.  
685 <https://doi.org/10.2136/sssaj1972.03615995003600060015x>  
686
- 687 Römken, M. J. M., & Prasad, S. N. (2006). Rain infiltration into swelling/shrinking/cracking  
688 soils. *Agricultural Water Management*, 86(1-2), 196–205.  
689 <https://doi.org/10.1016/j.agwat.2006.07.012>  
690
- 691 Slabaugh, J. D. (2006). *Final Report: Of Data from the Study of Sharkey Soils in the Lower*  
692 *Mississippi Valley*. US Department of Agriculture, Natural Resources Conservation Service,  
693 Little Rock, AR (65 pp.).  
694
- 695 Sprenger, M., Llorens, P., Cayuela, C., Gallart, F., & Latron, J. (2019). Mechanisms of  
696 consistently disjunct soil water pools over (pore) space and time. *Hydrology and Earth System*  
697 *Sciences*, 23(6), 2751–2762. <https://doi.org/10.5194/hess-23-2751-2019>  
698
- 699 Stewart, R. D., Abou Najm, M. R., Rupp, D. E., Lane, J. W., Uribe, H. C., Arumí, J. L., &  
700 Selker, J. S. (2015). Hillslope run-off thresholds with shrink–swell clay soils. *Hydrological*  
701 *Processes*, 29(4), 557–571. <https://doi.org/10.1002/hyp.10165>  
702
- 703 Stewart, R. D., Abou Najm, M. R., Rupp, D. E., & Selker, J. S. (2016a). A unified model for soil  
704 shrinkage, subsidence, and cracking. *Vadose Zone Journal*, 15(3).  
705 <https://doi.org/10.2136/vzj2015.11.0146>  
706
- 707 Stewart, R. D., Abou Najm, M. R., Rupp, D. E., & Selker, J. S. (2016b). Modeling multi-domain  
708 hydraulic properties of shrink-swell soils. *Water Resources Research*, 52(10), 7911–7930.  
709 <https://doi.org/10.1002/2016WR019336>  
710
- 711 Vargas, A. I., Schaffer, B., Yuhong, L., & Sternberg, L. D. S. L. (2017). Testing plant use of  
712 mobile vs immobile soil water sources using stable isotope experiments. *New*  
713 *Phytologist*, 215(2), 582–594. <https://doi.org/10.1111/nph.14616>

- 714  
715 Wassenaar, L. I., Hendry, M. J., Chostner, V. L., & Lis, G. P. (2008). High resolution pore water  
716  $\delta^2\text{H}$  and  $\delta^{18}\text{O}$  measurements by  $\text{H}_2\text{O}_{(\text{liquid})}$ - $\text{H}_2\text{O}_{(\text{vapor})}$  equilibration laser spectroscopy.  
717 *Environmental Science and Technology*, 42(24), 9262–9267. <https://doi.org/10.1021/es802065s>  
718
- 719 Weiler, M. & Flühler, H. (2004). Inferring flow types from dye patterns in macroporous soils.  
720 *Geoderma*, 120(1), 137–153. <https://doi.org/10.1016/j.geoderma.2003.08.014>  
721
- 722 Wells, R. R., DiCarlo, D. A., Steenhuis, T. S., Parlange, J. Y., Römkens, M. J. M., & Prasad, S.  
723 N. (2003). Infiltration and surface geometry features of a swelling soil following successive  
724 simulated rainstorms. *Soil Science Society of America Journal*, 67(5), 1344–1351.  
725 <https://doi.org/10.2136/sssaj2003.1344>  
726
- 727 Yasuda, H., Berndtsson, R., Persson, H., Bahri, A., & Takuma, K. (2001). Characterizing  
728 preferential transport during flood irrigation of a heavy clay soil using the dye Vitasyn Blau.  
729 *Geoderma*, 100(1–2), 49–66. [https://doi.org/10.1016/S0016-7061\(00\)00080-X](https://doi.org/10.1016/S0016-7061(00)00080-X)  
730